Electromagnetic Investigations of Aquifers in the Grand Brulé Coastal Area of Piton de la Fournaise Volcano, Reunion Island

by Bernard Robineau[a], Michel Ritz[b], Michel Courteaud[a], and Marc Descloitres[b]

Abstract

A geophysical survey was carried out on the eastern flank of Piton de la Fournaise volcano in the Grand Brulé area using combined audiomagnetotelluric (AMT) and time domain electromagnetic (TDEM) techniques. The aims of the present study were firstly to define the shallow geoelectrical structure, and subsequently to locate large bodies of ground water with anomalous electrical properties. Most of the AMT sites are isotropic across the entire observational bandwidth (7500-10 Hz), except for a few sites where static-shift effects are present. Joint one-dimensional interpretation of the TDEM and AMT data indicates basically three-layered structures with the following resistivity zones, progressing from the surface downward: (1) a resistive unsaturated surface layer of subaerial basaltic flows with a 2000 to 10,000 ohm-m resistivity, its base being approximately at mean sea level, (2) an intermediate-resistivity layer (100-250 ohm-m) 50-300 m thick, interpreted as being fresh-water-saturated basaltic formations, and (3) a low-resistivity layer of less than 15 ohm-m probably due to more saline water at depth and/or higher clay content in crushed materials. In the center of the study area, the results have also shown the presence of a prominent boundary dividing the area into a southern zone where the aquifer sequence is thin (60-100 m) and a northern zone corresponding to a relatively thick aquifer (>150 m). Geoelectrical models are compared with the available geological information given by two geothermic exploration drillings. The coastal drill hole gives a crucial information, i.e. the thick intermediate-resistivity layer in the northern part of Grand Brulé can be related to water-saturated alluvium deposits down to 200 m below sea level. AMT and TDEM soundings have revealed a major paleoalluvial drainage system buried under recent lava flows. A delimitation of sectors with different hydrogeological characteristics can be proposed.

Introduction

As part of a multidisciplinary program to evaluate groundwater potential in the lowlands of La Fournaise shield volcano (Figure 1) at Grand Brulé, electrical geophysical methods were applied to explore subsurface conditions. Aquifers are nothing but water-bearing geological formations and thus electrical methods have been the basic tools in water-bearing rocks exploration. In fact, the resistivity of a water-bearing formation is highly dependent upon porosity, degree of saturation, and water salinity (Keller and Frischknecht, 1966), and electrical surveys may be used to map aquifers and water quality zones. The inherent capabilities of the electrical geophysical methods to detect changes in water resistivity make them highly responsive to the fresh-/saline-water interface found in coastal and island regions.

Several authors have described the subject in detail (e.g., Fitterman, 1987; Hazell et al., 1988; Goldman et al., 1991). Conventional electrical resistivity surveying that has been used successfully for a variety of ground-water problems (e.g., Van Overmeeren, 1989; de Lima, 1993) is a tedious operation requiring large crews and voluminous measuring systems. Therefore, in this volcanic environment (with serious current injection problems), electromagnetic (EM) methods with large depth penetration capabilities were chosen. In the survey area a combination of two EM techniques has been employed to determine electrical resistivity stratification with depth namely, time domain electromagnetic (TDEM) and audiomagnetotelluric (AMT) methods. The main use of this work has been to detect, identify, and define aquifers by exploiting the expected large contrasts in resistivity between dry volcanic rocks (high resistivity), fresh-water-saturated rocks (intermediate resistivity), and salt-water contaminated basalt or clayey materials (low resistivity).

The study area (Figure 1) located on the eastern flank of La Fournaise volcano was restricted to a surface of about 10 km^2 because of limitations imposed by thick vegetation and rugged topography. The location of the TDEM/AMT survey conducted at Grand Brulé is shown in Figure 2. Also shown in Figure 2 are the location of drillholes which are pertinent to the discussion of the geophysical results.

[a]Laboratoire des Sciences de la Terre, Université de la Réunion, 97489 Saint Denis, La Réunion.
[b]ORSTOM, BP 1386, Dakar, Senegal.
Received February 1996, revised July 1996, accepted July 1996.

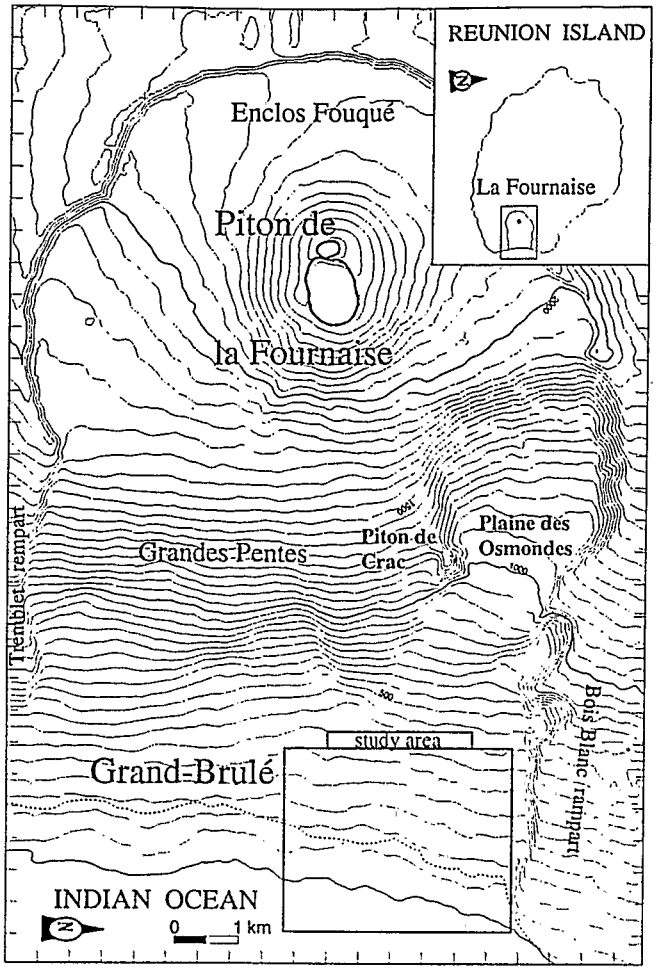

Fig. 1. Location map of study area and geomorphological features. The inset map shows the location of study area in Reunion Island.

Geological Background

Located along the eastern coast of Reunion Island, the remarkable uninhabited study area covers the northern part of Grand Brulé, a topographically depressed zone, filled with recent lavas of La Fournaise active shield volcano. Grand Brulé, bordered by two ramparts, has an overall 15% slope from the littoral cliff to the Enclos Fouqué open caldera (Figure 1). Looking at the geomorphological features, Grand Brulé presents some degree of asymmetry. Its northern part is characterized by a more eroded edge (Bois Blanc rampart) as mentioned by Kieffer (1990). Upward the 1000-1800 m steep slope feature, called Grandes Pentes, is disturbed to the north by a semicircular depressed zone. This zone named Plaine des Osmondes, runs from Bois Blanc rampart to Piton de Crac (Figure 1), both of them displaying older (phase III, Chevallier and Bachèlery, 1981) basaltic flows and pyroclastics. A collapsed calderic lobe is the only proposed interpretation for Plaine des Osmondes structure (Bachèlery, 1981). Although the geological map of Grand Brulé appears monotonous, with only a cover of recent to historic basaltic lava flows (Figure 2), its subsurface structure may present a more complex geometry. In fact, Enclos Fouqué/Grand Brulé U-shaped structure (Figure 1) is now unanimously considered as the result of an overall collapse (Duffield et al., 1982) or/and successive landslides on the volcano eastern flank (Chevallier and Bachèlery, 1981). Oceanographic surveys just offshore from Grand Brulé have clearly revealed several debris flows, with typical hummock features and scattered huge blocks (Lénat et al., 1989), that are related (Labazuy, 1991) to main volcanotectonic events of La Fournaise history (Bachèlery and Mairine, 1990). Consequently, important crushed and weathered (clayey) layers can be expected in Grand Brulé subsurface geology (landslide foot layers). Futhermore, submarine volcanics such as hyaloclastite should occur at great depths BSL because of the overall subsidence of this area.

Several geophysical investigations have been performed in Grand Brulé for a geothermic evaluation program. An extensive AMT survey (Benderitter and Gérard, 1984) has been carried out across Grand Brulé. Unfortunately, data are not published, but a conductive zone is seen at depths of .5-1 km beneath the northern coastal part of Grand Brulé and Bois Blanc rampart area. A major gravimetric anomaly has been partly mapped near the coast and modeled as a dense elliptic intrusive body. It has been found 800 m BSL by a deep exploration drilling at Grand Brulé well (GB well, Figure 2) and interpreted as a fossil magmatic chamber of a paleo Fournaise volcano (Rançon et al., 1989). Because of its depth and the AMT investigation range, this intrusion can hardly affect the subsurface geoelectric structure.

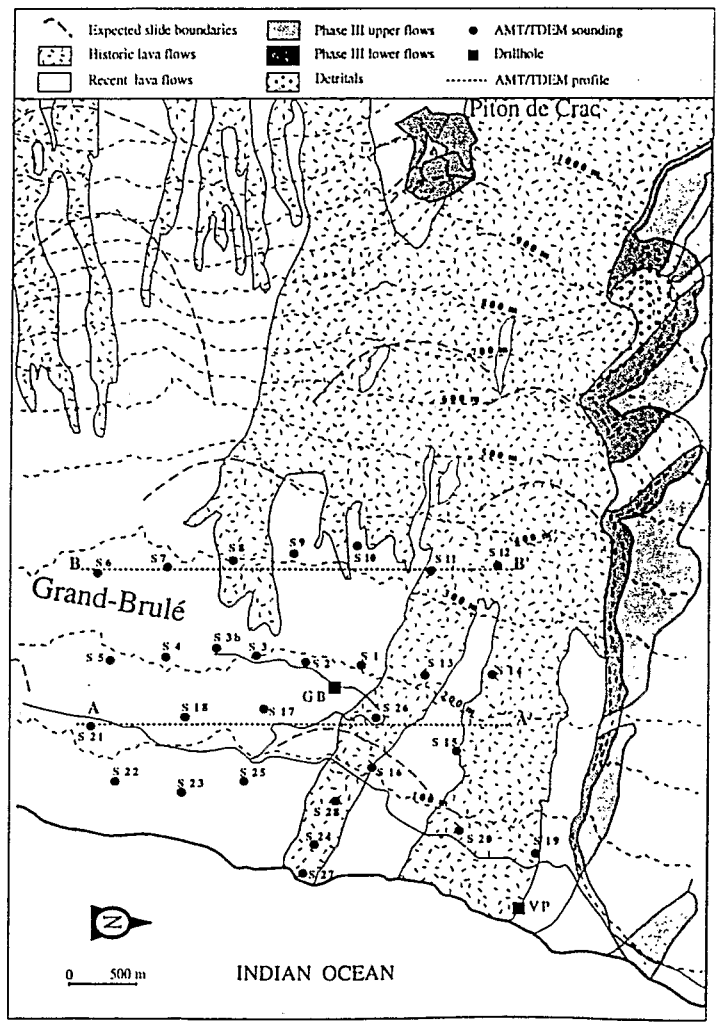

Fig. 2. Schematic geological map of survey area. The location of the TDEM/AMT sounding stations is shown by the solid circles with their site number. Lines A-A′ and B-B′ are the locations of the cross sections shown in Figure 6. The solid squares correspond to Grand Brulé (GB) and Vierge au Parasol (VP) wells drilled in the area. The elevation contours are in meters.

EM Methods

The TDEM method uses the interaction of a transient EM wave with the earth to determine the electrical resistivity of the earth as a function of depth. The TDEM system consists of a square large loop transmitter and a multiturn air coil receiver placed in the center of the loop. The TDEM method has been described in detail in a number of publications and monographs (e.g., Kaufman and Keller, 1983). In this survey, the data were collected with the Geonics TEM47 using two or three base frequencies. The field data acquired were interpreted using the interpretation software TEMIXGL (Interpex Limited, 1989).

AMT is a frequency-domain EM sounding technique in which variations in earth resistivity as a function of depth are measured. It consists of recording earth's surface natural EM field variations at different frequencies. The principles of the AMT method correspond to those of the magnetotelluric (MT) method (e.g., Vozoff, 1972), except that the measured signals are at higher frequencies and originate mainly from electrical discharges during lightning storms rather than from ionospheric or magnetospheric phenomena. The final data consist of the impedance tensor relating the horizontal electric and magnetic fields rotated into principal axes (TM and TE modes, perpendicular and parallel to the strike, respectively) and converted to phase and resistivity.

When the ground is to be investigated with the AMT method, the data are sometimes impaired by near-surface static distortion (Berdichevsky and Dmitriev, 1976; Jones, 1988). Static shift occurs if near-surface resistivity distribution is laterally inhomogeneous due to existing geological structures. A characteristic of such distortion is that, although it generates parallel offsets in the measured apparent resistivity curves, it does not operate on the phase of the AMT response. Locally rough topography can have the same effect. Interpretations based on those data will be erroneous. However, topographic effects for a slope (Wannamaker et al., 1986) appear relatively weak if breaks in slope are not large and the AMT response may be obtained accurately. Recent schemes to suppress the influence of near-surface resistivity contrasts involve the use of independent (e.g. TDEM) measurements of the near-surface resistivity (Sternberg et al., 1988; Pellerin and Hohmann, 1990) at exactly the same locations as AMT soundings. Such shallow data are used to construct a horizontally layered model, which in turn yields an apparent resistivity curve in the AMT method. The observed AMT curves are then shifted upward or downward so that they overlap with the apparent resistivity curve for the layered model at the high-frequency range. Since only magnetic field is measured in the TDEM method, instead of the magnetic and electric fields as in the AMT method, the TDEM data are considered to be free from the static effect (Qian and Pedersen, 1993). This correction scheme can be applied only to a horizontally layered resistivity structure. Sternberg et al. (1988) provided a relationship between AMT frequency and transient time. Thus, the time interval for our TDEM data from 7 μs to .71 ms will be equivalent to the frequency range 28,000-300 Hz, providing adequate overlap (more than one decade) with the AMT soundings.

Measurements were conducted with an Iris Instruments tensor AMT system, detecting two horizontal, time-varying, magnetic field components and their complementary horizontally orthogonal electric components across a frequency range from 1 to 7500 Hz. The maximum and minimum apparent resistivity and phase curves, azimuthal directions of the principal impedance, and skew values are computed directly for each frequency by means of a built-in microprocessor. The AMT data affected by static shift can be corrected using TDEM data.

Results

To obtain information on the distribution of aquifers at Grand Brulé, combined TDEM and AMT soundings were made at several locations (Figure 2). The TDEM data from the last few channels were rejected when they appeared to be noisy. Only two AMT soundings were largely influenced by near-surface static distortion (Jones, 1988). Such static bias was accounted for by TDEM data.

TDEM Results

Most of sites yield sounding curves with a monotonic decrease in apparent resistivity with time (except for sites 9-11). Such curve behavior undoubtedly proves the presence of a low-resistivity layer in the base of the section. Figure 3 shows four typical examples of TDEM sounding curves from locations close to the coast (sites 19 and 21) and farther inland (sites 1 and 11). The quantitative interpretation of the TDEM measurements is, however, hampered by the equivalence problem, which means that several different layered models may give practically the same resistivity curve. To choose the model that best represents the true conditions of the subsurface, auxiliary data such as well logs are needed. Unfortunately, no drilling evidence was available on the water table in the study area. Outside the survey area, the static water level is generally found at a few meters above mean sea level (MSL). As a first approach to help in resolving the ambiguity of the models, the depth to the interface between the expected aquifer and the overlying layer was fixed at approximately MSL.

The data were interpreted with the minimum number of layers that gave a good fit. The models, in the form of the equivalent resistivity vs. depth sections, for the four typical soundings are given in Figure 3. At some sites it was necessary to include a thin layer of very low resistivity within the top resistive layer to be consistent with the data.

AMT Results

The orthogonal AMT responses from most of AMT sites are coincident and reasonably one-dimensional (1-D) across the entire observational bandwidth, and appears to be little affected by static shift. Thus, it seems that the surface layers are seen as regionally homogeneous by individual AMT soundings. The determinant AMT response (Ranganayaki, 1984) from the sites free of such shifts is chosen to represent the data. Individual responses at all sites are not presented but typical apparent resistivity (ρa) and phase (ϕ) curves are shown in Figure 4. Exceptions to the 1-D character are sites 12 and 13 where a significant amount of parallel shift between the TM and TE amplitude curves is present. Other exceptions to the 1-D character are observed at some of our stations near the coast (sites 22-24, 27, and 28, Figure 2). The AMT responses at these stations are affected by the ocean (coastal effect, e.g. Ogawa, 1987). To see the coastal effect in AMT data, consider the responses of two-dimensional (2-D) theoretical models (Wannamaker et al., 1986; 1987) with and without ocean. The results from these models indicated that the TE mode is biased by the presence of the ocean. In contrast, the TM mode is relatively little affected by the ocean. The TM

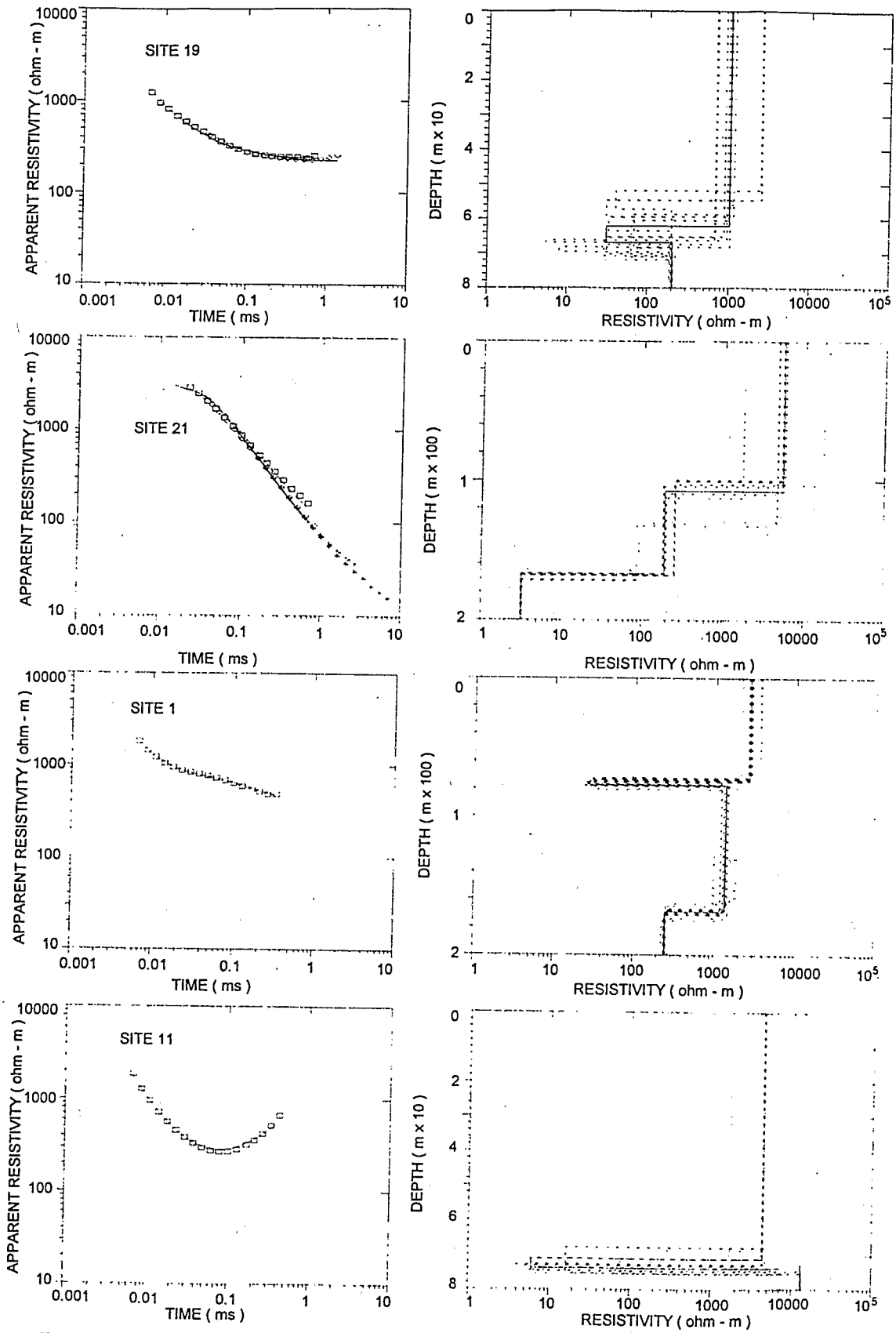

Fig. 3. TDEM sounding curves for four typical sites. Symbols in the left-hand graph are 3-frequency field data. Solid lines (in the left-hand graph) represent 3-frequency calculated responses for the best-fit models shown in the right-hand graph and dashed lines are the equivalent models. At some sites late-time data are rejected because the signal appeared to be noisy.

mode data at sites close to the coastline have then been emphasized in the 1-D modeling process.

Most of AMT responses (Figure 4) are characterized by high resistivity at high frequencies, a flatting more or less pronounced in the intermediate part of the curve (except at sites 9-11), and a decrease in apparent resistivity with decreasing frequency at the end of the measurement range. This typically results in a model with three layers. 1-D inversions (Jupp and Vozoff, 1975) of the determinant apparent resistivity and phase curves were conducted at each site.

The TDEM data provide good resistivity estimates for the near-surface material, which is poorly resolved from the AMT data because of a limited high-frequency information. Although the AMT data sound deeper than our TDEM system, the AMT models must also account for the effects of the near-surface material, because this material has significant influence on AMT responses, and incorporation of the uppermost zones into the model is important for correct modeling of the underlying regions (Berdichevsky and Dmitriev, 1976). The TDEM coverage can be used to provide near-surface control. Subsequently, the AMT soundings at high frequencies were interpreted using a layered model that matched the TDEM models as much as possible. The results of the 1-D modeling are illustrated for selected sites in Figure 4. A characteristic of all the soundings is the presence of a very conductive bottom layer with resistivities of less than 15 ohm-m. The RMS errors between the models and the observed data (Jupp and Vozoff, 1975) are less than 12%. All physical parameters of resistivity and thickness are reasonably well resolved except for some of them in the upper layers. The accuracy of our AMT models is difficult to evaluate. However, confidence in the models is inspired by the very small deviations between the TDEM and AMT apparent resistivity curves at frequencies higher than 300 Hz at most of the sites. There are no major disagreements between two completely different electromagnetic methods.

A comparison of the geophysically interpreted depths from sites 1 or 2 and 19 or 20 with the nearby lithologic logs (Figure 5) from wells GB and VP respectively (Figure 2) shows very general agreement. The depth of the better conductor (4 ohm-m) at site 1 agrees well with that of the subaerial and submarine basaltic lava flows with argillaceous intervals found in GB. Clearly the 190 ohm-m layer at site 19 is related to the sequence of basaltic materials with major alluvial beds composed of predominantly coarse-grained sediments ranging from pebbles to sands in VP. Discrepancies between the well logs and the TDEM/AMT results may be explained by the fact that (1) the soundings were not done over the drillhole locations and hence the depths to the interfaces are likely to be somewhat different, and (2) the resistivity contrasts depend not only on change in lithology but also on the presence of water-filled fractures and the presence of clay within each sequence.

Cross Sections

Using the inversion results from the combination of the TDEM and AMT data, two resistivity-versus-depth cross sections, both trending north south, were constructed (AA′ and BB′, Figure 2) to obtain a better understanding of the electrical structure under the study area. In general, the cross sections (Figure 6) show a good consistency from site to site and a pattern of smoothly varying structures. Cross sections indicate the following layers progressing from the surface downward: (1) a

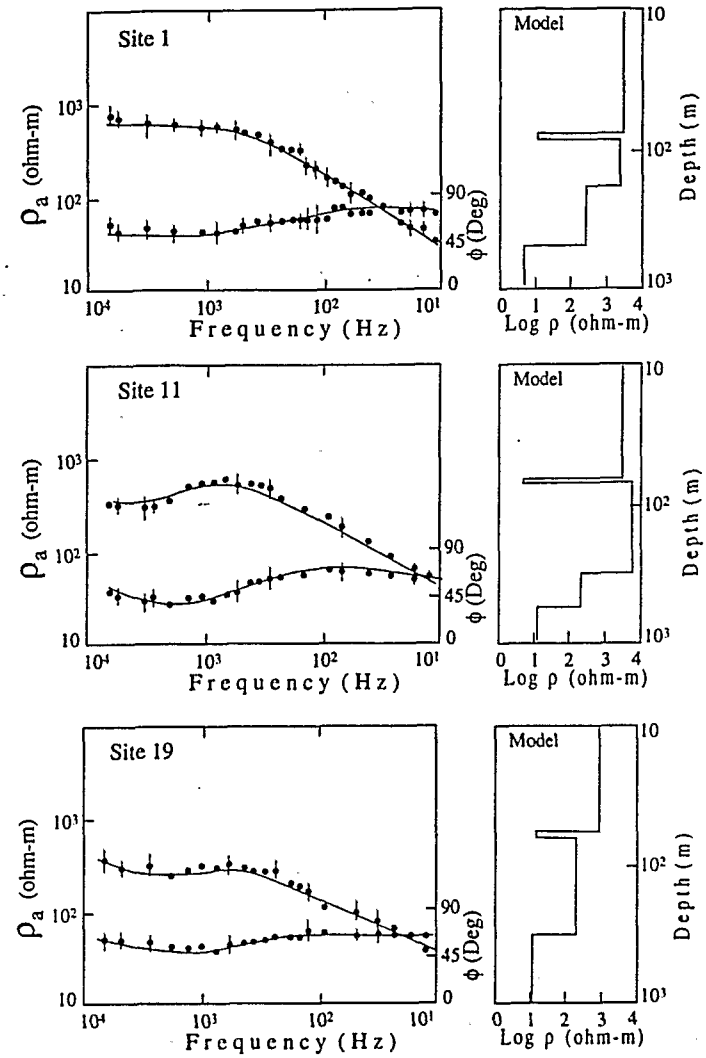

Fig. 4. Examples of determinant apparent resistivity and phase sounding data at sites 1, 11, and 19 (symbols in the left-hand graph) with error bars (95% confidence intervals, not plotted when smaller than the symbols). Solid lines in the left-hand graph are the responses to the best-fit model (right-hand graph) from 1-D inversion. The upper part of the models is obtained from the results of the TDEM interpretations.

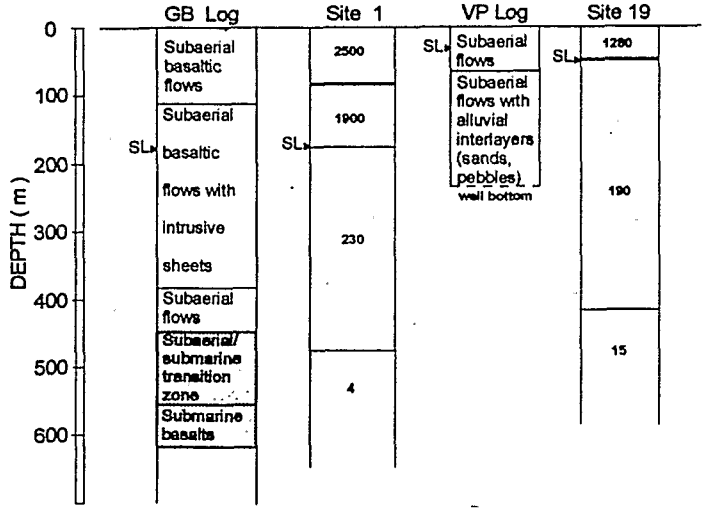

Fig. 5. Comparison between layered resistivity sounding interpretation from sites 1 and 19 and lithologic logs from Grand Brulé (GB) and Vierge au Parasol (VP) wells, respectively. The shaded layers in GB log correspond to the occurrence of important argillaceous beds (Rançon et al., 1989).

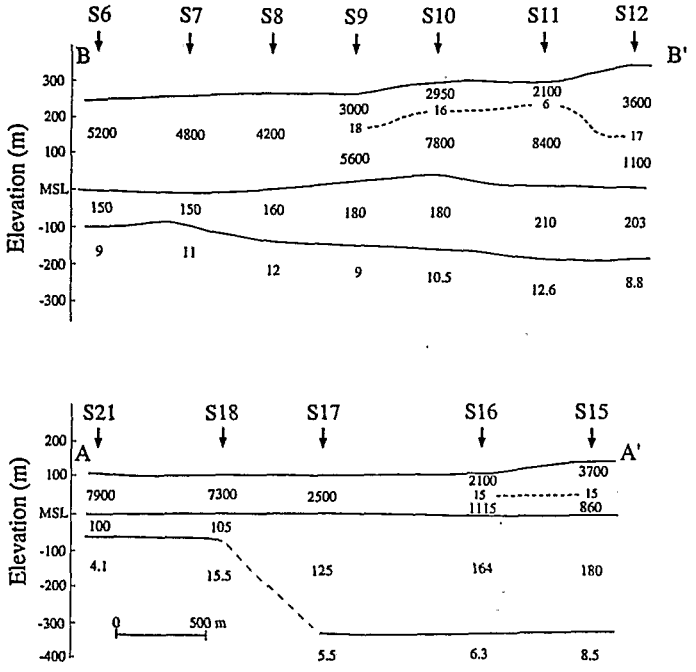

Fig. 6. Composite 1-D geoelectrical cross sections using TDEM/AMT data for Grand Brulé profiles A-A′ and B-B′ (see Figure 2 for profile location). Near-surface resistivity values were constrained by the TDEM coverage. Boundaries between layers are marked by solid lines, and the resistivity of the layers in ohm-m are indicated by numbers. The thin horizontal dash indicates a thin conductive layer within the top resistive layer observed at TDEM sites 16 and 15 along profile A-A′ and at TDEM sites 9, 10, 11, and 12 along profile B-B′.

resistive surface layer of which the base is located approximately at MSL, (2) an intermediate-resistivity layer 50-300 m thick, and (3) a low-resistivity basement less than 15 ohm-m.

The top layer with a resistivity of 2000-10,000 ohm-m reflects dry or slightly wet subaerial basaltic flows. At some sites, additional conductive layers of less than 20 ohm-m, 4-8 m thick, appear within the resistive layer. They are probably indicative of lahar and/or tuffaceous interbeds in the section.

The second layer has resistivities in the range 100 to 250 ohm-m. At nearly all sites we found that the well-resolved top of the 100-250 ohm-m layer approximately coincides with sea level (except for sites 8-11 on profile B-B′, Figure 6). On profile A-A′ between sites 18 and 17, the thickness of this layer varies in an abrupt manner from 50 m to about 300 m. A prominent discontinuity is suggested north of site 18. On profile B-B′, thickness variations are more gradual; the thickness of the layer increases slowly northward from 100 m to 200 m. The resistivity range for layer two is too low for dry basaltic rocks and must represent rocks saturated with fresh water. It likely constitutes the fresh-water-bearing zone recharged by high rainfall areas. This surface is similar to the water table which is typically marked by an abrupt decrease in resistivity. Regions of perched water tables would be expected at sites 9 and 10 on profile B-B′, where the layer top is clearly above MSL.

For the third layer, the resistivity ranges from 4 to 15 ohm-m, which points to clayed zones or a higher ground-water salinity, or both. The persistence of this conductive layer from the coast to farther inland is best explained by formations having significant amounts of clay (see well GB). However, sea-water intrusion cannot be ruled out as the cause of the low resistivities observed at sites located close to the coast. In the absence of additional information, we assume that the conductor constitutes a clayey, poorly permeable basement, likely underlying saline water close to the coast.

Contour Map

The identification of large bodies of ground water being the main goal of the present study, a contour map (Figure 7) has also been prepared of aquifer depth below sea level (BSL) derived from the 1-D resistivity models. As previously mentioned, the aquifer mapping is based on the measurements of the depth to the interface associated with the bottom of the intermediate-resistivity (100 to 250 ohm-m) layer interpreted to reflect the fresh-water-bearing zone. It will be noted that the top of this layer is generally at MSL and was associated with the water table. Thus, the depth to the interface coincides approximately with the aquifer thickness. Although the aquiferous zone appears thick enough over the entire area, the contour map (Figure 7) shows that this aquifer is highly variable in thickness, being thinnest in the southern part with thicknesses increasing from about 60 m close to the coast to 120 m and more inland. The northern part corresponds to a relatively thick aquifer, but shows an inverse relationship between thicknesses/depths and elevations. The thicknesses vary from about 300 m near the coast to 200 m in highland, except for small circular zones of higher thickness at an elevation of about 150 m (near sites 1, 16, and 17). The boundary between the two zones is marked by steep gradients, particularly near the coast. These depth gradients probably indicate a major structural boundary. Note that in the northeast part of the region mapped, the aquifer's base dips to the northeast, and the aquifer sequence becomes thicker near the coast (thicker than 300 m at sites 19 and 20). Such an area is a candidate for ground-water exploration.

Discussion and Conclusions

Based upon (1) the geoelectic cross sections obtained (Figure 6), (2) the trends observed on the aquifer BSL contour map (Figure 7), and (3) the available geological information from two wells VP and GB (Figure 2), a hydrogeological interpretation can be proposed for Grand Brulé subsurface. At least three major zones (Figure 7) can be distinguished.

1. Zone A: A Paleoalluvial System

This interpretation is based upon the lithological information given by the VP coastal well (Figure 5). Under 60 m of aerial lava flows are found alluvial deposits down to 200 m BSL. There is a great similarity between these alluvial formations and the 300 m thick intermediate-resistivity second layer from the nearest soundings 19 and 20. The geophysical continuity observed landward along profiles AA′ (site 15) and BB′ (site 12), and the morphology of the basal conductor top (Figure 7) in zone A, suggest that alluvium belongs probably to a buried paleovalley. This paleoriver should present an E-W direction parallel to the topographic gradient, as in most cases of actual rivers of La Fournaise volcano. Furthermore, the 800-1100 ohm-m layer (Figure 6) observed above sea level at sites 12 and 15 have a smaller resistivity value than usual dry basaltic flows and could represent dry alluviums. Note that the 300 m BSL bottom of the alluvial layer (Figure 7) implies a syn-to post-deposit subsidence. The L1 (Figure 7) prominent boundary between zone A and the southern part of our study area represents the location of the

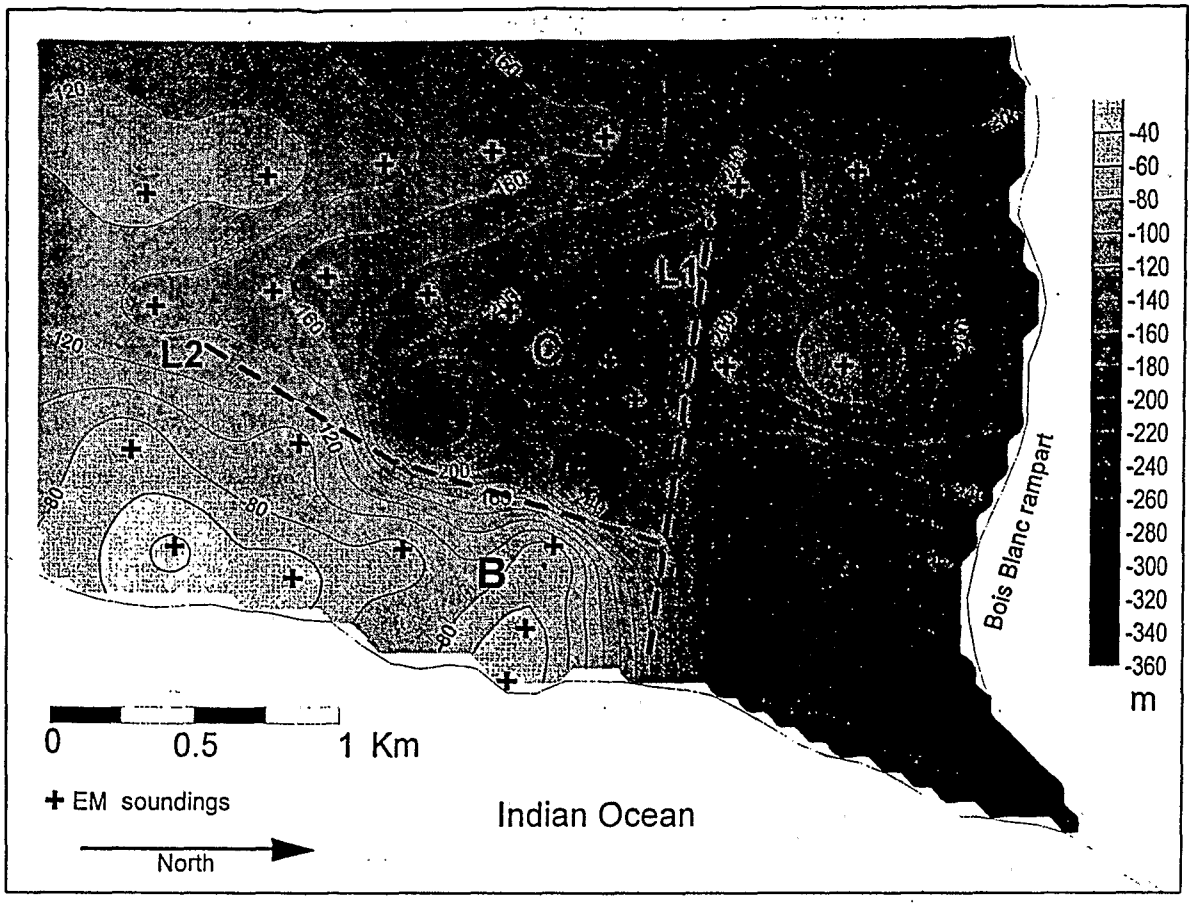

Fig. 7. Contour map of fresh-water depth (BSL).

southern bank of the paleoriver. This alluvial system is interpreted as a drainage structure recharged by high rainfall areas (Plaine des Osmondes, a good part of the Enclos Fouqué caldera, and even lateral zones). Because of the steep gradient upland, and the expected lower (compared to surrounding basaltic flows) permeability of alluvial deposits, the coastal aquifer may be characterized by a high hydraulic pressure. This could explain the great depth of the basal conductor at coastal sites 19 and 20 (Figure 7), the fresh-/salt-water interface being tilted or even driven offshore.

2. Zone B: A Coastal Aquifer

The subsurface geoelectrical structure of this zone presents the typical geometry of a volcanic coastal aquifer in equilibrium with sea water, i.e. the fresh-water/sea-water interface usually has a low landward dip (Ecker, 1976). In zone B, all EM soundings show (1) low-resistivity values (< 5 ohm-m) of the basal conductor which are probably associated with sea-water-saturated basaltic rocks. Note that these values are similar to those of Hawaii (6 ohm-m) inferred from an EM study (Lienert, 1991), (2) a gentle deepening of the conductor top landward, and (3) an aquifer thickness compatible with the Ghyben-Herzberg principle (Kashef, 1983). Furthermore, transition layers with resistivities of about 10 ohm-m (probably brackish water) have been modeled at sites 22 and 23 (Figure 2) between the aquifer and the sea-water-saturated basement. The low dipping of the fresh-/salt-water wedge in zone B indicates a high-permeability aquifer with a low piezometric gradient.

3. Zone C: A Volcanic Aquifer with a Poorly Permeable Substratum

This zone covers the upper ⅔ of the southern part of the study area (Figure 7). Its lower limit corresponds to the maximum extent of the sea-water intrusion inland. Zone C aquifer does not rest in equilibrium on a conventional lavic sea-water-saturated formation. As a matter of fact, the depth of the conductor top does not increase with elevation but the contrary, and resistivity values of the conductive basement are higher (approximately 10 ohm-m). Comparison of well GB lithologic log (Figure 5) and models from neighbor soundings (sites 1, 2, and 26) shows that zone C conductive substratum can be related to argilized volcanic materials that act as a poorly permeable layer underlying the aquifer. The criteria that are necessary to discriminate zone C proceed from hydrogeologic implications: (1) depth of the low-permeability substratum, (2) hydraulic pressure conditions landward, and (3) hydrodynamic characteristics of the water-saturated layer. For example, the southern L2 diffuse boundary (Figure 7) marks out the contact of the fresh-/salt-water wedge with a shallower substratum. On the contrary, L2 becomes a sharp limit northward between zones B and C and expresses a sudden dip of the fresh-/salt-water interface. In that case, it is necessary to suppose less favorable hydrodynamic characteristics of the zone C aquifer and a higher water pressure in the northern part of the study area.

The TDEM/AMT survey shows the potential of using complementary geophysical techniques for rapid mapping of subsurface resistivities and for detecting large bodies of ground

water with anomalous electrical properties in the complicated terranes of the Grand Brulé volcanic field, where drillhole lithologic information is few. The TDEM method is to be more useful for detection of shallowest resistivity structures whereas the AMT soundings provide better resistivity estimates for the detection of deeper layers. The AMT soundings can be influenced by near-surface static distortion (Berdichevsky and Dmitriev, 1976) caused by surficial inhomogeneous structures. However, using TDEM data (Pellerin and Hohmann, 1990) the AMT static shift can be properly corrected.

The results of the study have led to the identification of the aquiferous zone within the study area. This zone varies in thickness from place to place, but the highest potential for groundwater exploration is clearly the northeast part of Grand Brulé where the aquifer is thickest and probably consists of water-saturated alluvial sediments, deposited in a deep and narrow paleovalley now buried under the recent lava flows of La Fournaise volcano.

Acknowledgments

This work was supported by a Conseil Général de la Réunion research grant in the framework of La Fournaise Massif Hydrogeological Program directed by Prof. J. Coudray. We are grateful to Y. Albouy, P. Mourgues, and J. Descloitres for their field contribution.

References

Bachèlery, P. 1981. Le Piton de la Fournaise (Ile de la Réunion). Etude volcanologique, structurale et pétrologique. Ph.D. thesis, Univ. Clermont-Ferrand II, France. 215 pp.

Bachèlery, P. and P. Mairine. 1990. Evolution morpho-structurale du Piton de la Fournaise depuis .53 Ma. In: Le volcanisme de l'île de la Réunion. J.F. Lénat (ed.), Paris. pp. 213-242.

Benderitter, Y. and A. Gérard. 1984. Geothermal study of Reunion Island: Audiomagnetotelluric survey. J. Volcanol. Geotherm. Res. v. 20, pp. 311-332.

Berdichevsky, M.N. and V.I. Dmitriev. 1976. Basic principles of interpretation of magnetotelluric sounding curves. In: Geoelectric and Geothermal Studies (East-Central Europe, Soviet Asia). KAPG Geophys. Monogr., Akademiai Kiado, Budapest, A. Adam (ed.). pp. 165-221.

Chevallier, L. and P. Bachèlery. 1981. Evolution structurale du volcan actif du Piton de la Fournaise, Ile de la Réunion. Bull. Volcanol. v. 45, pp. 287-298.

De Lima, O.A.L. 1993. Geophysical evaluation of sandstone aquifers in the Recôncavo-Tucano Basin, Bahia-Brazil. Geophysics. v. 58, pp. 1689-1702.

Duffield, W.A., L. Stieltjes, and J. Varet. 1982. Huge landslide blocks in the growth of Piton de la Fournaise, La Réunion, and Kilauea volcano, Hawaii. J. Volcanol. Geotherm. Res. v. 12, pp. 140-160.

Ecker, A. 1976. Groundwater behaviour in Tenerife, volcanic island (Canary Island, Spain). J. Hydrol. v. 28, pp. 73-86.

Fitterman, D.V. 1987. Examples of transient sounding for ground-water exploration in sedimentary aquifers. Ground Water. v. 25, pp. 685-692.

Goldman, M., D. Gilad, A. Ronen, and A. Melloul. 1991. Mapping of seawater intrusion into the coastal aquifer of Israel by the time domain electromagnetic method. Geoexploration. v. 28, pp. 153-174.

Hazell, J.R.T., C.R. Cratchley, and A.M. Preston. 1988. The location of aquifers in crystalline rocks and alluvium in Northern Nigeria using combined electromagnetic and resistivity techniques. Q. J. Eng. Geol. v. 21, pp. 159-175.

Interpex Limited. 1989. TEMIX User's Manual. Interpex Ltd.

Jones, A.G. 1988. Static shift of magnetotelluric data and its removal in a sedimentary basin environment. Geophysics. v. 53, pp. 967-978.

Jupp, D.L.B. and K. Vozoff. 1975. Stable iterative methods for the inversion of geophysical data. Geophys. J.R. Astron. Soc. v. 50, pp. 333-352.

Kaufman, A.A. and G.V. Keller. 1983. Frequency and Transient Soundings. Elsevier, Amsterdam.

Kashef, A.I. 1983. Harmonizing Ghyben-Herzberg interface with rigorous solutions. Ground Water. v. 21, pp. 152-159.

Keller, G.V. and F.C. Frischknecht. 1966. Electrical Methods in Geophysical Prospecting. Pergamon, NY.

Kieffer, G. 1990. Grands traits morphologiques de l'île de la Réunion. In: Le volcanisme de l'île de la Réunion. J.F. Lénat (ed.), Paris. pp. 75-114.

Labazuy, P. 1991. Instabilités au cours de l'évolution d'un édifice volcanique en domaine intraplaque océanique: le Piton de la Fournaise (Ile de la Réunion). Ph.D. thesis, Univ. Clermont-Ferrand II, France. 260 pp.

Lénat, J.F., P. Vincent, and P. Bachèlery. 1989. Sea-beam mapping of the offshore continuation of an active basaltic volcano: Piton de la Fournaise (Reunion Island, Indian Ocean). Structural and geomorphological interpretation. J. Volcanol. Geotherm. Res. v. 36, pp. 1-36.

Lienert, B.R. 1991. An electromagnetic study of Maui's last active volcano. Geophysics. v. 56, pp. 972-982.

Pellerin, L. and G.W Hohmann. 1990. Transient electromagnetic inversion: A remedy for magnetotelluric static shifts. Geophysics. v. 55, pp. 1242-1250.

Qian, W. and L.B. Pedersen. 1993. Spatial averaging of the vertical magnetic field in central-loop configuration. Geophysics. v. 58, pp. 1507-1510.

Rançon, J., P. Lerebour, and T. Augé. 1989. The Grand Brulé exploration drilling: New data on the deep framework of the Piton de la Fournaise volcano, part 1: lithostratigraphic units and volcano-structural implications. J. Volcanol. Geotherm. Res. v. 36, pp. 113-127.

Ranganayaki, R.P. 1984. An interpretive analysis of magnetotelluric data. Geophysics. v. 49, pp. 1730-1748.

Sternberg, B.K., J.C. Washburne, and L. Pellerin. 1988. Correction for the static shift in magnetotellurics using transient electromagnetic soundings. Geophysics. v. 53, pp. 1459-1468.

Van Overmeeren, R.A. 1989. Aquifer boundaries explored by geoelectrical measurements in the coastal plain of Yemen: A case of equivalence. Geophysics. v. 54, pp. 38-48.

Vozoff, K. 1972. The magnetotelluric method in the exploration of sedimentary basins. Geophysics. v. 37, pp. 98-141.

Wannamaker, P.E., J.A. Stodt, and L. Rijo 1986. Two-dimensional topographic responses in magnetotellurics modeled using finite elements. Geophysics. v. 51, pp. 2131-2144.

Wannamaker, P.E., J.A. Stodt, and L. Rijo 1987. A stable finite element solution for two-dimensional magnetotelluric modeling. Geophys. J.R. Astron. Soc. v. 88, pp. 277-296.